



# Preparation and characterization of organic-soluble acetylated starch nanocrystals

Yue Xu<sup>a,b</sup>, Wanqiang Ding<sup>a</sup>, Ji Liu<sup>a</sup>, Ya Li<sup>a</sup>, John F. Kennedy<sup>c</sup>, Qun Gu<sup>a</sup>, Shuangxi Shao<sup>a,b,\*</sup>

<sup>a</sup> Ningbo Key Laboratory of Polymer Materials, Ningbo Institute of Material Technology and Engineering, Chinese Academy of Sciences, Ningbo, Zhejiang 315201, PR China

<sup>b</sup> Institute of Applied Chemistry, Ningbo University of Technology, Ningbo, Zhejiang 315016, PR China

<sup>c</sup> Chembiotech Laboratories, Institute of Advanced Science and Technology, 5 The Croft, Buntsford Drive, Stoke Heath, Bromsgrove, Worcs, B60 4JE, UK

## ARTICLE INFO

### Article history:

Received 20 October 2009

Received in revised form 9 January 2010

Accepted 11 January 2010

Available online 18 January 2010

### Keywords:

Acetylation

Starch nanocrystals

Degree of substitution

Organic-soluble

Solubility

Hydrophobicity

## ABSTRACT

Efficient procedures for the preparation of organic-soluble starch nanocrystal (SN) derivatives have been established with different degrees of substitution (DS). The resulting acetylated starch nanocrystals exhibit much improved solubility in common organic solvents such as *N,N*-dimethylformamide, acetone, carbon tetrachloride and toluene. The obtained nanocrystals were characterized by means of the FT-IR, <sup>1</sup>H NMR and X-ray photoelectron spectroscopic techniques. When compared with the hydrophobic performance of the unmodified starch nanocrystals, that of acetylated starch nanocrystals significantly increased according to the contact angle measurement results. X-ray diffraction reveals that the crystal-line structure of acetylated starch nanocrystals was changed from style A to style V. The platelet-like starch nanocrystals become sphere-shaped after modification and the size increases compared to the ungrafted particles as revealed by transmission electron microscopic results. They are versatile precursors to nanoparticle-based copolymers, composites, and metal ligands.

Crown Copyright © 2010 Published by Elsevier Ltd. All rights reserved.

## 1. Introduction

Among carbohydrate polymers, starch is an abundant, inexpensive, naturally renewable, and biodegradable polysaccharide, which has been widely investigated for the potential manufacture of products such as water-soluble pouched for detergents and insecticides, flushable lines and bags, and medical delivery systems and devices (Chi et al., 2008; Fishman, Coffin, Konstance, & Onwulata, 2000; Ma, Yu, & Kennedy, 2005).

There is currently a considerable interest in nanocomposites materials. As most of the present polymers used for nanocomposite preparation are synthetic materials, their processability, biocompatibility, and biodegradability are much more limited than those of natural polymers. Since starch is the cheapest biopolymer available, and it is totally biodegradable, starch nanocrystals obtained from waxy maize starch have been used as fillers in a polymeric matrix which lead to a desired reinforcing effect (Dufresne, 2008; Helene Angellier, 2005, 2006). For the processing of composite materials, starch nanocrystals are used in the form of aqueous suspensions and the matrices are latexes. The main obstacle for the use of starch nanocrystals as a reinforcing phase in a wide variety of polymers is its poor solubility in organic solvents. A surfactant can be used to disperse starch nanocrystals in a nonpolar solvent

when it is used for cellulose whiskers (Bonini et al., 2002; Heux, Chauve, & Bonini, 2000), however, a large amount of the surfactant is needed to maintain the stability of the suspension. Such a drawback hinders the use of this technique for composites processing in organic solvents. The use of DMF of big dielectric constant and of tuncin whiskers of medium wettability is capable of controlling the stability of the suspension (AziziSamir, Alloin, Sanchez, ElKissi, & Dufresne, 2004). Although such compounds may be used in starch nanocrystals, it would limit the use of other organic solvents. Therefore, physical or chemical modifications on starch nanocrystals have been extensively studied, among which the surface chemical modification is a sound approach and a lot of relevant research work has been done (Labet, Thielemans, & Dufresne, 2007; Thielemans, Belgacem, & Dufresne, 2006; Tsuji & Kawaguchi, 2005). In the past years, it has been reported that some polymers such as poly(tetrahydrofuran), poly(propylene glycol) monobutyl ether, poly(carprolactone) and poly(styrene) (Chang & Peter, 2009; Labet et al., 2007; Shiwei Song, Pan, & Wang, 2008) were used to chemically modify the properties of starch nanocrystals. However, the polymer modified starch nanocrystals aggregation still exists and the solubility with organic solutions is not satisfactory. Starch nanocrystals with short grafting agents was also reported (Tsuji & Kawaguchi, 2005), but the grafting extent is not sufficient to induce a partial solubilization of starch molecules located at the surface of the nanocrystals.

In this paper, we report the fabrication of organic-soluble acetylated starch nanocrystals with different degrees of substitution by adopting a simple approach. The acetylated starch nanocrystals

\* Corresponding author. Address: Ningbo Key Laboratory of Polymer Materials, Ningbo Institute of Material Technology and Engineering, Chinese Academy of Sciences, Ningbo, Zhejiang 315201, PR China. Tel./fax: +86 574 87081521.

E-mail address: [sxshao@nimte.ac.cn](mailto:sxshao@nimte.ac.cn) (S. Shao).

could reduce their surface energy and showed good solubility in organic solvents such as acetone, chloroform and ethyl acetate. Also, the acetylated starch nanocrystals exhibited unique hydrophobicity. The excellent properties of the acetylated starch nanocrystals are useful in applications in packaging industry and as nano-reinforcements.

## 2. Materials and methods

### 2.1. Materials

Corn starch was obtained from Zhu Cheng Xing Mao Corn Developing Co., Ltd. (Shandong, China). Glacial acetic acid, sulfuric acid, acetic anhydride, dimethyl sulphoxide (DMSO), methanesulphonic acid (MSA) and other chemicals were purchased from Sinopharm Chemical Reagent Co., Ltd. (Shanghai, China). All of the chemicals are of analytical grade and used without further purification.

### 2.2. Corn starch nanocrystals preparation

The starch nanocrystals were prepared according to the procedure described in the literature (Angellier, Choinsard, Molina-Boisseau, Ozil, & Dufresne, 2004). The typical preparation method is as follows: 36.725 g of starch were mixed with 250 ml of 3.16 M  $\text{H}_2\text{SO}_4$  at 40 °C and were poured into a flask with a continuous horizontal and circular stirring (100 rpm) for 5 days. The suspension was washed by successive centrifugations with distilled water until it reached neutrality. Then the solvent exchange was done from distilled water to acetone by successive centrifugations at 8000 rpm and 10 °C for 15 min.

### 2.3. Preparation of the acetylated starch nanocrystals

The resulting starch nanocrystals were used after the acetone evaporated totally. 2.5 g of the starch nanocrystals and 15 ml of glacial acetic acid were placed in a 250 ml three-neck flask. After treatment under ultrasonic conditions for 5 min, 30 ml of acetic anhydride was added to the mixture. After stirring for a few minutes, 0.3 g of methanesulphonic acid was added to the reactor. The reaction mixture was stirred at 400 rpm for 5 h. By keeping the reaction temperature at 40, 50, and 65 °C, respectively, esters with three different substitutions were obtained.

### 2.4. Determination of the solubility of the starch nanocrystals and acetylated starch nanocrystals

Both the starch nanocrystals and acetylated starch nanocrystals (DS = 2.45) were dispersed in *N,N*-dimethylformamide, acetone, carbon tetrachloride and other common solvents (list in Table 1) at a concentration of 5 mg/ml at room temperature. Pictures were taken to illustrate the solubility after modification in some typical



**Fig. 1.** Pictures of solubility tests: (1) starch nanocrystals and (2) acetylated starch nanocrystals (DS 2.45) were dissolved in (A) *N,N*-dimethylformamide, (B) acetone, (C) carbon tetrachloride and (D) toluene immediately after stopping stirring, (1') starch nanocrystals and (2') acetylated starch nanocrystals were placed 48 h later.

organic solvents (as shown by Fig. 1). The acetylated starch nanocrystals were well dissolved in most of organic solvents, while the starch nanocrystals become a suspension state after stirring. Even after 48 h, the suspension still shows a marked turbidity and the acetylated starch nanocrystals remain transparent.

### 2.5. Characterization

#### 2.5.1. Fourier transform infrared (FT-IR) spectroscopy

FT-IR spectra were recorded using a Nicolet 6700 spectrometer. The starch nanocrystals and acetylated starch nanocrystals samples were collected using the KBr pellet method. The resolution was 4  $\text{cm}^{-1}$  and the total scans were 32. The samples were dried at 60 °C in the vacuum oven before measurement.

#### 2.5.2. X-ray photoelectron spectrometry

XPS spectra of the samples were recorded on a Kratos AXIS UltraDLD photoelectron spectrometry using monochromatized Al  $K\alpha$  radiation at 1486.6 eV. XPS beam angle of 75° to the specimen surface was used. Survey spectra were an average of three scans acquired at pass energy of 160 eV and resolution of 1.5 eV/step. High-resolution spectra of O 1s and C 1s were an average of 4 scans acquired at pass energy of 10 eV and resolution of 0.05 eV/step. Dwell time was 100 ms for survey scans, 150 ms for O 1s and C 1s scans. A neutralizer gun with filament current of 2.1 A, filament bias of 1 V and a charge balance of 2.6 V was used to reduce charging of the samples while scanning. Binding energy corrections were made by referencing spectra to the C–C bond to 284.8 eV. The starch nanocrystals and acetylated starch nanocrystals powders

**Table 1**

Solubility of starch nanocrystal (a) and acetylated SN (DS 2.45) (b) in organic solvent.

| Solubility |                                |                   |                 |                         |            |
|------------|--------------------------------|-------------------|-----------------|-------------------------|------------|
|            | <i>N,N</i> -Dimethylformamide  | Dichloromethane   | Tetrahydrofuran | Cyclohexane             | Ethanol    |
| a          | —                              | —                 | —               | —                       | —          |
| b          | +                              | +                 | +               | —                       | —          |
|            | Carbon tetrachloride           | Trichloromethane  | Petroleum ether | Pyridine                | Acetone    |
| a          | —                              | —                 | —               | —                       | —          |
| b          | +                              | +                 | —               | +                       | +          |
|            | <i>N</i> -Methyl-2-pyrrolidone | Dimethylsulfoxide | Toluene         | Acetic acid ethyl ester | Ethylether |
| a          | —                              | +                 | —               | —                       | —          |
| b          | +                              | +                 | +               | +                       | —          |

were dried in vacuum oven at 60 °C prior to analysis. Quantitative XPS analysis was performed using CasaXPS software (version 2.3.14). Relative atomic concentrations were determined by subtracting a Shirley-type background.

### 2.5.3. Contact angle measurements

Contact angles were measured at room temperature using a Dataphysics OCA20 Contact Angle system. The drop volume was about 6  $\mu\text{L}$ , and dropped carefully onto the films for five different positions of the same sample.

The starch nanocrystals and acetylated starch nanocrystals samples for contact angle measurements were heated at 60 °C in DMSO (5 g/L) to obtain clear solutions, and cooled at room temperature before casting onto glass slide and being dried at 85 °C for 5 h in vacuum oven.

The dispersive and polar contributions of the surface energy of the starch nanocrystals before and after modification were evaluated by applying the Owens–Wendt approach (Owens & Wendt, 1969). (The work of adhesion is replaced by the Young equation.)

$$\gamma_L(1 + \cos \theta) = 2\sqrt{\gamma_L^D \gamma_S^D} + 2\sqrt{\gamma_L^P \gamma_S^P} \quad (1)$$

where  $\gamma$ ,  $\gamma^D$ , and  $\gamma^P$  is the total, dispersive, and polar surface energy, respectively; subscripts L and S refer to the liquid drop (L) and the solid surface (S); and  $\theta$  denotes the contact angle between the solid substrate and the liquid drop. The liquid surface tensions were taken from the literature (Adao, Saramago, & Fernandes, 1999; Wang, Zhang, Abidi, & Cabrales, in press). The above parameters are listed below. Water: ( $\gamma^D$ , 21.8 (mJ/m<sup>2</sup>);  $\gamma^P$ , 51.0 (mJ/m<sup>2</sup>);  $\gamma^{\text{Total}}$ , 72.8 (mJ/m<sup>2</sup>); ethylene glycol: ( $\gamma^D$ , 29.0 (mJ/m<sup>2</sup>);  $\gamma^P$ , 19.0 (mJ/m<sup>2</sup>);  $\gamma^{\text{Total}}$ , 48.0 (mJ/m<sup>2</sup>); diiodomethane: ( $\gamma^D$ , 49.5 (mJ/m<sup>2</sup>);  $\gamma^P$ , 1.3 (mJ/m<sup>2</sup>);  $\gamma^{\text{Total}}$ , 50.8 (mJ/m<sup>2</sup>).

### 2.5.4. Nuclear magnetic resonance (NMR) spectroscopy analysis

The typical <sup>1</sup>H NMR spectrum was recorded using a Bruker AV 400 spectrometer at 25 °C with a resonance frequency of 400 MHz. The starch nanocrystals and acetylated starch nanocrystals were dissolved in deuterated dimethyl sulphoxide (DMSO-d<sub>6</sub>) at room temperature to obtain solutions. The analysis was carried out at 25 °C.

<sup>1</sup>H NMR could be used to determine the DS of the acetylated starch nanocrystals as it is used to evaluate starch. Based on the report (Teramoto & Shibata, 2006), when the substitution of the acetylated starch was lower than 2.5 (DS < 2.5), it could be calculated by the following Eq. (2). However, based on the report (Elo-maa et al., 2004), when the substitution of the acetylated starch was above 2.5 (DS > 2.5), it could be calculated by the following Eq. (3).

$$\text{DS}_{\text{low}} = 4A/(3B + A) \quad (2)$$

$$\text{DS}_{\text{high}} = 7A/3C \quad (3)$$

where A is sum of areas of methyl protons at 1.8–2.2 ppm, B is OH protons and H-1 protons of anhydroglucose unit moiety observed at more than 4.7 ppm, and C is the sum of areas of seven protons in anhydroglucose unit observed at higher than 3.95 ppm. According to Eqs. (2) and (3), we could know that when the reaction temperature was 40, 50 and 65 °C, the degree of substitution was 0.16, 0.99 and 2.45, respectively.

### 2.5.5. Wide-angle X-ray diffraction (WARD)

The X-ray diffraction patterns of the samples dried at ambient temperature were recorded by using a Bruker D8-Advanced diffractometer at 40 kV and 30 mA.

### 2.5.6. Transmission electron microscopy (TEM)

Transmission electron micrographs of the starch nanocrystals and acetylated starch nanocrystals were taken with a Hitachi 7650 transmission electron microscope with an acceleration voltage of 80 kV. Deposited starch nanocrystals were negatively stained with a 2% aqueous solution of uranyl acetate, and the acetylated starch nanocrystals were deposited on a carbon-coated grid without any treatments.

## 3. Results and discussion

### 3.1. Solubility of the acetylated starch nanocrystals

Table 1 lists the solubility of the starch nanocrystals and acetylated starch nanocrystals (DS = 2.45) in organic solvents. As shown in Table 1, starch nanocrystal could only dissolve in DMSO. When the DS value was 2.45, the acetylated starch nanocrystals could be soluble in halogenated hydrocarbons, aromatic solvents and polar solvents such as *N,N*-dimethylformamide, acetone, carbon tetrachloride and toluene (as shown in Fig. 1), and no precipitation was observed upon prolonged standing. This might be due to the high degree of substitution on the starch nanocrystal surface containing hydrophobic groups. The hydrogen bonds are disrupted by the hydrophobic methyl groups and the solubility was enhanced by the acetyl groups. The solubility analysis indicates that acetylation dramatically changed the solubility of the starch nanocrystals, thus the acetylated starch nanocrystals could be more compatible with hydrophobic polymers when it was used as a reinforcing phase.

### 3.2. Structure and properties of the starch nanocrystals and different DS of the acetylated starch nanocrystals

The surface modification was confirmed by the results of the FT-IR, XPS, and contact angle measurements. We used <sup>1</sup>H NMR technique to detect the detail chemical structures of the acetylated starch nanocrystals; X-ray diffraction measurements were performed to detect the crystalline structures of the starch nanocrystals and different DS of the acetylated starch nanocrystals; the morphologies of both modified and unmodified particles were observed by means of the TEM technique.

The FT-IR spectra (Fig. 2) of the starch nanocrystals and acetylated starch nanocrystals with different substitutions showed clear

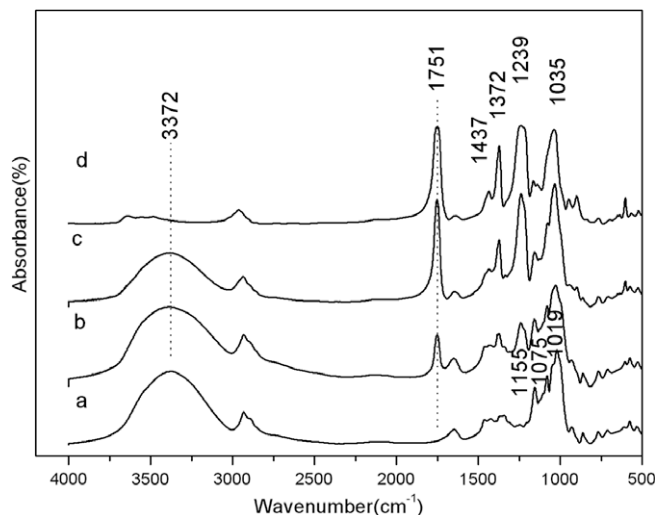


Fig. 2. FT-IR spectra for (a) starch nanocrystal and acetylated starch nanocrystals: (b) DS 0.16, (c) DS 0.99, and (d) DS 2.45.

traces of modification. In the spectra of the starch nanocrystals, a broad band due to hydrogen bonded hydroxyl groups appeared at  $3372\text{ cm}^{-1}$ . With the increase of substitution, the hydroxyl group bands gradually decreased in intensity and almost disappeared when the DS value reached 2.45. In other words, most of the hydroxyl groups were involved in the reaction. There were several discernible absorption bands of the starch nanocrystals at 1155, 1079, and  $1019\text{ cm}^{-1}$ , attributable to C–O bond stretching (Fang, Fowler, Sayers, & Williams, 2004). Compared to the starch nanocrystals, the acetylated starch nanocrystals with different substitutions showed a strong ester signal at  $1751\text{ cm}^{-1}$ , and it increased in intensity with the rise of substitution degree. At the same time, new absorption bands at 1437, 1372, and  $1239\text{ cm}^{-1}$  could be assigned to  $\text{CH}_3$  asymmetrical deformation vibration,  $\text{CH}_3$  symmetrical deformation vibration and carbonyl C=O stretch vibration, respectively. The appearance of these new absorptions suggests that the acetylated starch nanocrystals products were formed during the esterification process.

The XPS analysis provided more quantitative data of the level of surface modification as shown in Fig. 3. The peaks at around 531 and 287 eV correspond to 1s orbital electrons of oxygen and carbon atoms in the low resolution spectra (Fig. 3). In other words, carbon and oxygen atoms are the main components in both unmodified and modified starch nanocrystals. In the high-resolution carbon spectra (Fig. 3), the carbon signal could be resolved into several

component that represent the local environments of carbon atoms (C–C and C–H or C–O or O–C–O or O–C=O). For all of the samples, the four components could be categorized according to the bonds, in which C was involved in unmodified and modified starch nanocrystal structures. The unmodified and modified starch nanocrystals exhibited contributions of each type of carbon atoms but at different proportions. The ratio of carbon atoms with two bonds to oxygen to carbon atoms with one bond to oxygen (O–C–O/C–O) is 0.21, which is very close to the theoretical value of 0.2 predicted according to the formula of pure starch  $(\text{C}_6\text{H}_{10}\text{O}_5)_n$ . The presence of carboxylic groups may indicates the formation of lipids (Rindlav-Westling & Gatenholm, 2003), resulting from the oxidation of the reducing end groups of the starch. After modification, the proportions of each carbon atom were significantly different. In particular, the proportions of O–C=O bonds increased obviously after grafting. These results can explain the presence of acetyl groups after modification.

The presence of acetyl groups after modification was further confirmed by the results of contact angle measurements. When adding a droplet of distilled water, it was quickly spread out on the starch nanocrystal surface, giving the low contact angle value of  $36.8^\circ$  (Fig. 4). Because the starch nanocrystal surface was full of OH-rich macromolecules, it could form hydrogen bonds in water. A significant increase of contact angle with water was observed after grafting. The contact angles for the acetylated starch

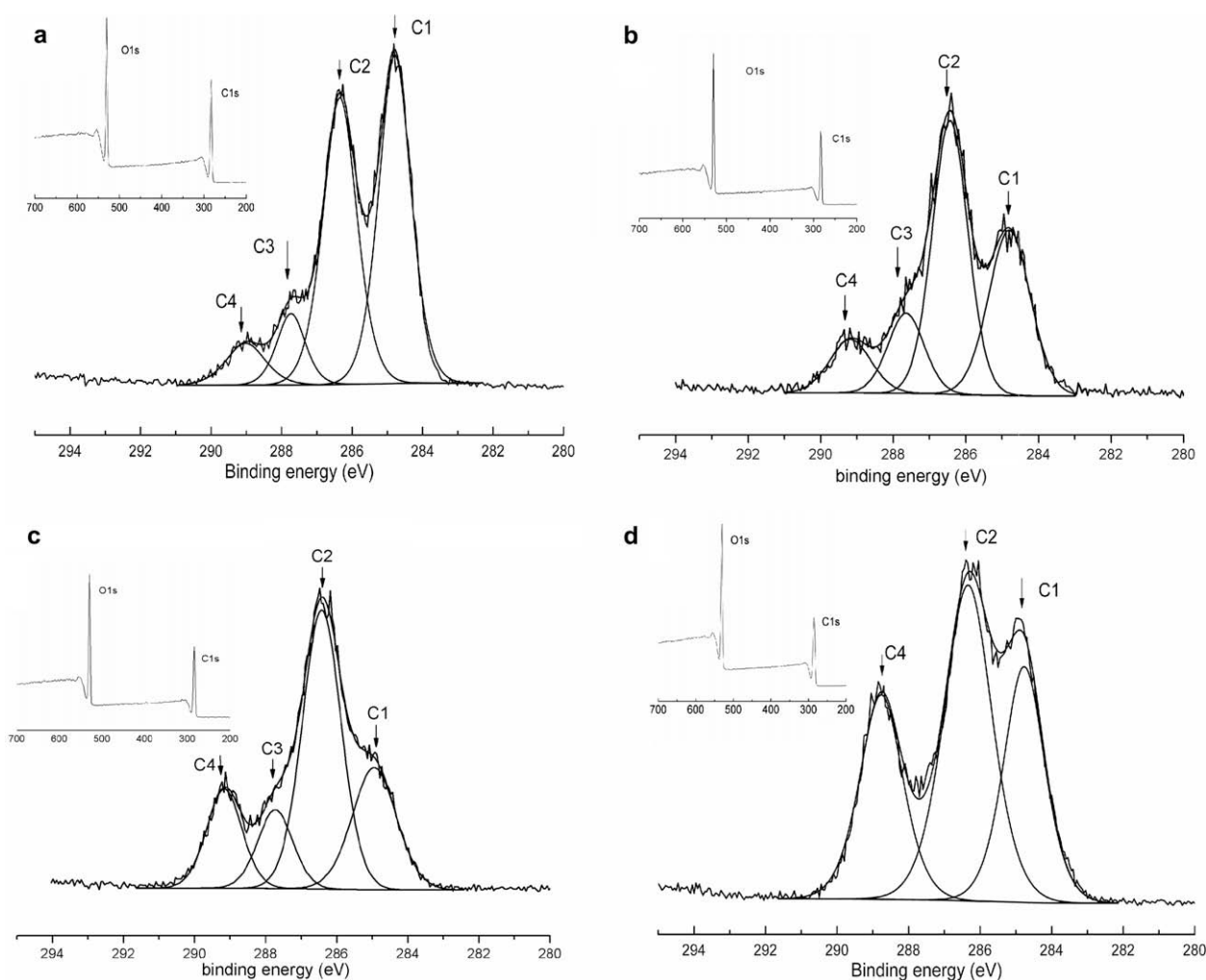


**Fig. 3.** Decomposition of the C 1s signal into its constituent for (a) starch nanocrystals and acetylated starch nanocrystals: (b) DS 0.16, (c) DS 0.99, (d) DS 2.45. Insets: XPS wide scans from 1s orbital electrons of oxygen and carbon atoms.



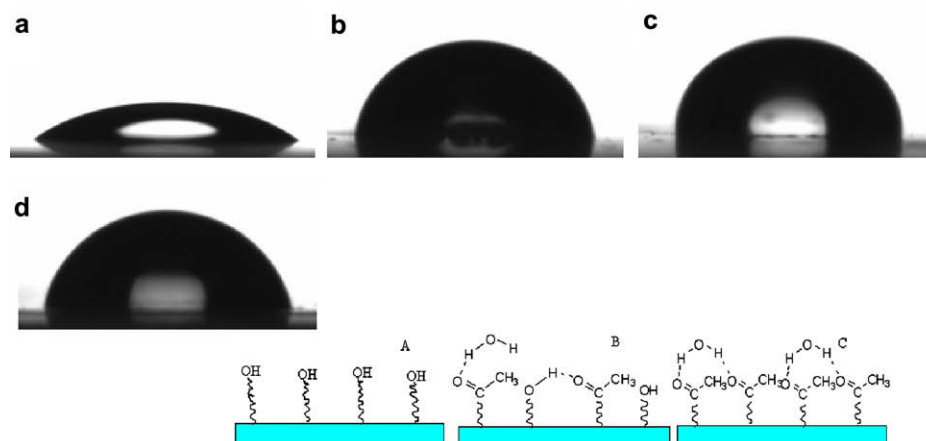


**Fig. 4.** Photographs of water drop on the surface of (a) unmodified starch nanocrystal and acetylated starch nanocrystals: (b) DS 0.16, (c) DS 0.99, and (d) DS 2.45. Schematic illustration of contact angle measurements: (A) unmodified starch nanocrystal and acetylated starch nanocrystals: (B) DS 0.16/0.99, and (C) DS 2.45.

nanocrystals with DS = 0.16, 0.99 and 2.45 were 77.8°, 88.8° and 67.9°, respectively, as shown in Fig. 4. Since the surfaces of the acetylated starch nanocrystals with DS = 0.16 and 0.99 possessed only a small portion of acetyl groups and a lot of hydroxyl groups, the carbonyl groups could form intramolecular hydrogen bonds with hydroxyl groups on the acetylated starch nanocrystal surface, with a droplet of water added on the acetylated starch nanocrystal surface, methyl groups might play an important role in generating a hydrophobic interface. In the photographs of the acetylated starch nanocrystals with DS = 2.45 (close to the theoretical DS value of 3), the carbonyl groups could form intermolecular hydrogen bonds with water molecules, so the contact angle of this sample was smaller than those of the acetylated starch nanocrystals with lower DS values. Hydrophilicity is one of the most prominent features of esterified starch nanocrystals determined by contact angle measurement (Fig. 4). The replacement of hydrophilic hydroxyl groups by acetyl groups reduced the hydrophilicity. Further experiments were performed with ethylene glycol and diiodomethane to determinate the values of the surface energy of all the samples, and the results are shown in Table 2. For ethylene glycol, which is polar liquid, was deposited on the same substrates. For diiodomethane, which is a nonpolar liquid, the contact angle values were barely lower for modified substrates. The unmodified starch nanocrystals exhibited a polar surface energy as high as the dispersive one, as expected from an OH-rich surface, and similar values were reported in the literature (Labet et al., 2007; Thielemans et al., 2006; Tsuji & Kawaguchi, 2005). It is observed that the polar contribution to the surface energy was reduced after grafting, but the sample with DS = 0.99 gave the lowest value, which can also be understood from Fig. 4. When the DS value reaches to 2.45, the surface is full of acetyl group, but when the DS value is 0.99, the carbonyl groups form intramolecular hydrogen bonds with hydroxyl groups, which made the surface stand a lot of methyl group. The dispersive surface energy values were decreased with the rise in the DS value, indicating that the morphology of the acetylated

starch nanocrystals with DS = 2.45 was the most stable sample. The surface energy reflects efficient surface modifications in agreement with the results of FT-IR and XPS investigations.

The assignments of  $^1\text{H}$ -shifts for starch nanocrystals are summarized at the end of the paragraph and the  $^1\text{H}$  NMR spectra of the acetylated starches are presented in Fig. 5. via the esterification process, acetyl groups were introduced into the starch nanocrystals, and the signal due to protons of methyl groups appeared at 1.8–2.2 ppm. For the acetylated starch nanocrystals with DS = 0.16 and 0.99, the peaks characteristics of anhydroglucose unit could be still observed owing to the fact that only a portion of hydroxyl groups participated in the modification, as revealed by the signals in 3.29–3.65 ppm range. There were some hydroxyl groups in low-DS acetylated starch nanocrystals, similar resonances of protons were therefore observed for hydroxyl groups at 5.44 and 4.58 ppm when compared to the starch nanocrystals. In the spectrum of the acetylated starch nanocrystals with DS = 2.45 and 0.99, there were new peaks at 5.26, 5.18, 4.76, and 4.22–4.32 ppm, which could be ascribed to the H-3, H-1, H-2, and H-6,6' signals, respectively. All of these signals were from the acetylated starch nanocrystals. Signals of hydroxyl groups in anhydroglucose units disappeared for the acetylated starch nanocrystals with a DS value of 2.45, and the chemical environments of protons were totally different when compared to the starch nanocrystals.  $^1\text{H}$  NMR(starch nanocrystals) (400 MHz, DMSO- $d_6$ ,  $\delta$ ): 5.1 (w, 1H, H-1), 3.31 (s, 1H, H-2), 3.96 (w, 1H, H-3), 3.37 (s, 1H, H-4), 3.08 (w, 1H, H-4 end group), 3.60 (s, 1H, H-5), 3.65 (s, 2H, H-6,6'), 5.42 (m, 1H, H-2), 5.44 (m, 1H, H-3).

According to Fig. 6, the starch nanocrystals showed diffraction peaks at  $2\theta = 15.2^\circ$ ,  $17.1^\circ$ ,  $18.0^\circ$ , and  $23.0^\circ$ , indicating the scattering pattern for the A allomorph (Katopo, Song, & Jane, 2002; Matveev et al., 2001; Van Soest, Hulleman, de Wit, & Vliegenthart, 1996). The crystalline structure of the acetylated starch nanocrystals with DS = 0.16 kept intact although the diffraction peaks were less well-defined due to a few part of the hydroxyl groups being substituted.

**Table 2**

Contact angle and surface energy contributions of (a) unmodified starch nanocrystal and acetylated starch nanocrystals: (b) DS 0.16, (c) DS 0.99, and (d) DS 2.45.

| Sample | Contact angle $\theta$ |                 |               | $\gamma_s^p$ (mJ/m $^2$ ) | $\gamma_s^d$ (mJ/m $^2$ ) | $\gamma_s$ (mJ/m $^2$ ) |
|--------|------------------------|-----------------|---------------|---------------------------|---------------------------|-------------------------|
|        | Water                  | Ethylene glycol | Diiodomethane |                           |                           |                         |
| a      | 36.8                   | 31.8            | 41.6          | 31.9                      | 29.1                      | 61.0                    |
| b      | 77.8                   | 42.7            | 36.9          | 6.6                       | 30.3                      | 36.9                    |
| c      | 88.8                   | 47.3            | 37.5          | 2.7                       | 29.8                      | 32.5                    |
| d      | 68.9                   | 57.7            | 40.3          | 15.4                      | 21.1                      | 36.5                    |

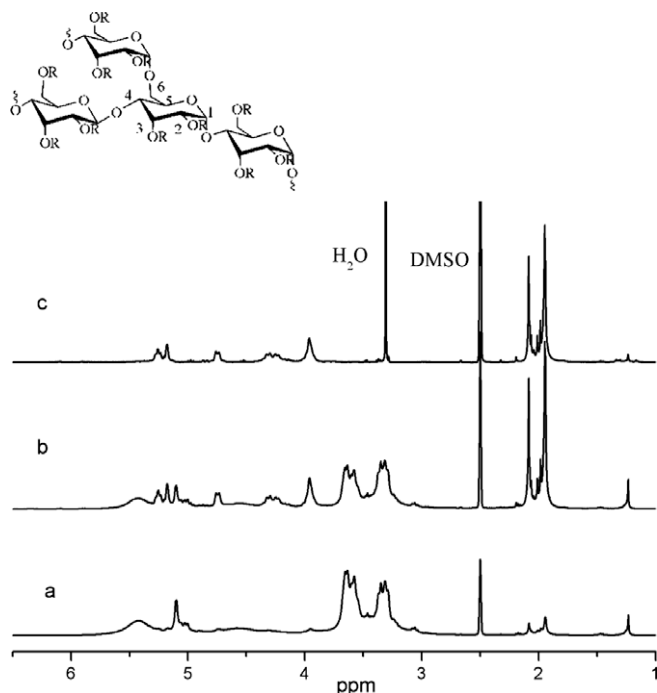


Fig. 5.  $^1\text{H}$  NMR spectra of acetylated starch nanocrystals: (a) DS 0.16, (b) DS 0.99, and (c) DS 2.45.

It is observed that the acetylated starch nanocrystals with DS = 0.99 showed a profile similar to that of the unmodified starch nanocrystals, but the former had a new peak at  $2\theta = 9.7^\circ$ , which appeared diffusion peaks of the acetylated starch nanocrystals (Chi et al., 2008). However, as the DS value increased to 2.45, the acetylated starch nanocrystals destroyed A-style crystallinity of the starch nanocrystals, and exhibited the V-style crystallinity, as confirmed by the detection of wide peaks at  $2\theta = 9.2^\circ$  and  $20.7^\circ$ . The X-ray diffraction results indicated that after esterification, the V-style crystallinity structure of the acetylated starch nanocrystals was formed.

Transmission electron micrographs of the unmodified and modified nanocrystals (DS = 2.45) are shown in Fig. 7a and b, respectively. The morphology of starch nanocrystals obtained after acid hydrolysis was almost the same as that reported previously (Putaux, Molina-Boisseau, Momauro, & Dufresne, 2003), which were platelet-like nanoparticles with the diameter in the range of 20–40 nm. They were found to aggregate, a result due to hydrogen

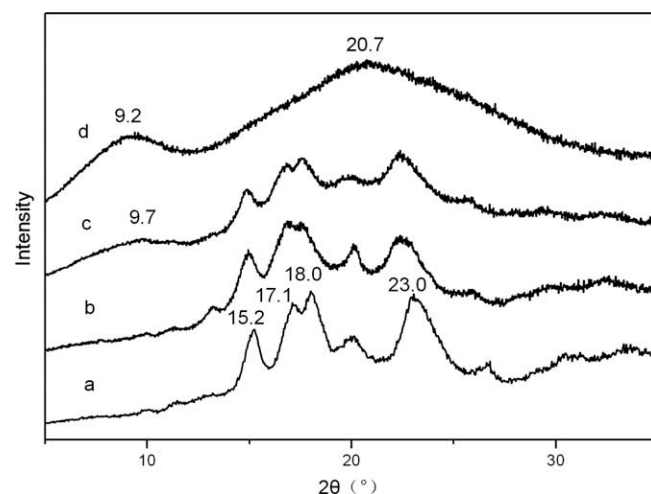


Fig. 6. X-ray diffraction patterns of (a) starch nanocrystal and acetylated starch nanocrystals: (b) DS 0.16, (c) DS 0.99, and (d) DS 2.45.

bond interactions via the surface hydroxyl groups. The platelet-like particles of the unmodified starch nanocrystals became spherical ones after modifications (Fig. 7b) with the diameter ranged from 63 to 271 nm. It seems that the platelet-like geometrical form of the starch nanocrystals was preserved although the particle sizes increased and they were more individualized. The acetylated starch nanocrystals with a substitution degree of 2.45 still had a certain amount of hydroxyl groups in the nanoparticles to form inter- and intramolecular hydrogen bonds, which led to forming most of the sphere-shaped particles connecting together through a thread. Sphere-shaped particles seem to be coated with a layer because their sizes increased compared to the ungrafted particles. This modification resulted in a pronounced effect because agglomeration was invisible after surface modifications.

#### 4. Conclusions

Starch nanocrystals were successfully modified with acetic anhydride of different DS. Structures of the starch nanocrystals and different DS of the acetylated starch nanocrystals were characterized by FT-IR, XPS, NMR and contact angle measurements. The X-ray diffraction results indicated that, after esterification, a V-style crystallinity structure of the acetylated starch nanocrystals was formed. The structure of the acetylated starch nanocrystals illustrated that the modified starch nanocrystals

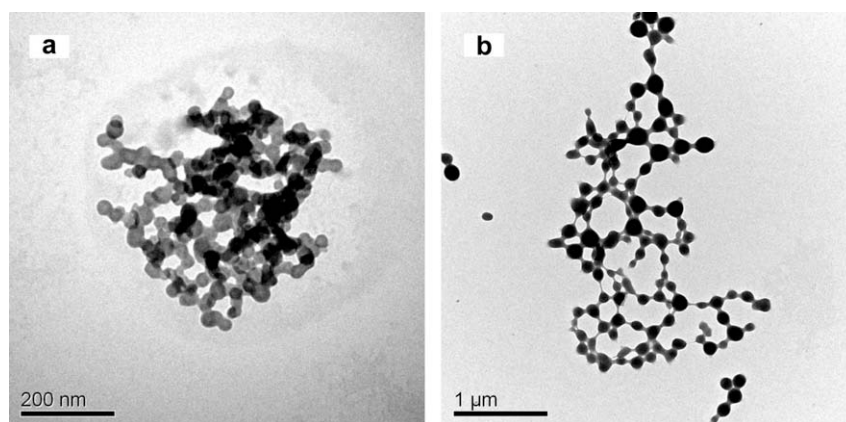


Fig. 7. Transmission electron micrographs of (a) unmodified and (b) DS 2.45 acetylated starch nanocrystals.

exhibited enhanced solubility and hydrophobicity, which was confirmed by solubility analysis and contact angle measurements. These advantages clearly pave the way to potential applications in many fields, for example, as can be used as sizing agents in the textile industry, as a surface glue in paper industry, and as thickeners in the film and fiber industry.

## Acknowledgements

This work was financially supported by the Key Projects in the National Science & Technology Pillar Programs (Contract No. 2007BAE28B06).

## References

- Adao, M. H. V. C., Saramago, B. J. V., & Fernandes, A. C. (1999). Estimation of the surface properties of styrene-acrylonitrile random copolymers from contact angle measurements. *Journal of Colloid and Interface Science*, 217(1), 94–106.
- Angellier, H., Choisnard, L., Molina-Boisseau, S., Ozil, P., & Dufresne, A. (2004). Optimization of the preparation of aqueous suspensions of waxy maize starch nanocrystals using a response surface methodology. *Biomacromolecules*, 5(4), 1545–1551.
- AziziSamir, M. A. S., Alloin, F., Sanchez, J. Y., ElKissi, N., & Dufresne, A. (2004). Preparation of cellulose whiskers reinforced nanocomposites from an organic medium suspension. *Macromolecules*, 37(4), 1386–1393.
- Bonini, C., Heux, L., Cavaillé, J.-Y., Lindner, P., Dewhurst, C., & Terech, P. (2002). Rodlike cellulose whiskers coated with surfactant: A small-angle neutron scattering characterization. *Langmuir*, 18(8), 3311–3314.
- Chi, H., Xu, K., Wu, X., Chen, Q., Xue, D., Song, C., et al. (2008). Effect of acetylation on the properties of corn starch. *Food Chemistry*, 106(3), 923–928.
- Dufresne, A. (2008). Polysaccharide nano crystal reinforced nanocomposites. *Canadian Journal of Chemistry-Revue Canadienne De Chimie*, 86(6), 484–494.
- Elomaa, M., Asplund, T., Soininen, P., Laatikainen, R., Peltonen, S., Hyvärinen, S., et al. (2004). Determination of the degree of substitution of acetylated starch by hydrolysis, <sup>1</sup>H NMR and TGA/IR. *Carbohydrate Polymers*, 57(3), 261–267.
- Fang, J. M., Fowler, P. A., Sayers, C., & Williams, P. A. (2004). The chemical modification of a range of starches under aqueous reaction conditions. *Carbohydrate Polymers*, 55(3), 283–289.
- Fishman, M. L., Coffin, D. R., Konstance, R. P., & Onwulata, C. I. (2000). Extrusion of pectin/starch blends plasticized with glycerol. *Carbohydrate Polymers*, 41(4), 317–325.
- Helene Angellier, J.-L. P. S. M.-B. D. D. A. D. (2005). Starch nanocrystal fillers in an acrylic polymer matrix. *Macromolecular Symposia*, 221(1), 95–104.
- Helene Angellier, S. M.-B. A. D. (2006). Waxy maize starch nanocrystals as filler in natural rubber. *Macromolecular Symposia*, 233(1), 132–136.
- Heux, L., Chauve, G., & Bonini, C. (2000). Nonfloculating and chiral-nematic self-ordering of cellulose microcrystals suspensions in nonpolar solvents. *Langmuir*, 16(21), 8210–8212.
- Katopo, H., Song, Y., & Jane, J.-I. (2002). Effect and mechanism of ultrahigh hydrostatic pressure on the structure and properties of starches. *Carbohydrate Polymers*, 47(3), 233–244.
- Labet, M., Thielemans, W., & Dufresne, A. (2007). Polymer grafting onto starch nanocrystals. *Biomacromolecules*, 8(9), 2916–2927.
- Ma, X., Yu, J., & Kennedy, J. F. (2005). Studies on the properties of natural fibers-reinforced thermoplastic starch composites. *Carbohydrate Polymers*, 62(1), 19–24.
- Matveev, Y. I., van Soest, J. J. G., Nieman, C., Wasserman, L. A., Protserov, V. A., Ezernitskaja, M., et al. (2001). The relationship between thermodynamic and structural properties of low and high amylose maize starches. *Carbohydrate Polymers*, 44(2), 151–160.
- Owens, D. K., & Wendt, R. C. (1969). Estimation of the surface free energy of polymers. *Journal of Applied Polymer Science*, 13(8), 1741–1747.
- Peter, R., & Chang, F. A. Y. C. A. D. J. H. (2009). Effects of starch nanocrystallite-graft-polycaprolactone on mechanical properties of waterborne polyurethane-based nanocomposites. *Journal of Applied Polymer Science*, 111(2), 619–627.
- Putaux, J. L., Molina-Boisseau, S., Momaur, T., & Dufresne, A. (2003). Platelet nanocrystals resulting from the disruption of waxy maize starch granules by acid hydrolysis. *Biomacromolecules*, 4(5), 1198–1202.
- Rindlav-Westling, A., & Gatenholm, P. (2003). Surface composition and morphology of starch, amylose, and amylopectin films. *Biomacromolecules*, 4(1), 166–172.
- Shiwei Song, C. W., Pan, Zelin., & Wang, Xiufen. (2008). Preparation and characterization of amphiphilic starch nanocrystals. *Journal of Applied Polymer Science*, 107(1), 418–422.
- Teramoto, N., & Shibata, M. (2006). Synthesis and properties of pullulan acetate. Thermal properties, biodegradability, and a semi-clear gel formation in organic solvents. *Carbohydrate Polymers*, 63(4), 476–481.
- Thielemans, W., Belgacem, M. N., & Dufresne, A. (2006). Starch nanocrystals with large chain surface modifications. *Langmuir*, 22(10), 4804–4810.
- Tsuji, S., & Kawaguchi, H. (2005). Surface chemical modification of waxy maize starch nanocrystals. *Langmuir*, 21(6), 2434–2437.
- Van Soest, J. J. G., Hulleman, S. H. D., de Wit, D., & Vliegenthart, J. F. G. (1996). Crystallinity in starch bioplastics. *Industrial Crops and Products*, 5(1), 11–22.
- Wang, S., Zhang, Y., Abidi, N., & Cabrales, L. (2009). Wettability and surface free energy of graphene films. *Langmuir*, 25(18), 11078–11081.